

# Image Cover Sheet

**CLASSIFICATION**

UNCLASSIFIED

**SYSTEM NUMBER**

506936



**TITLE**

ELECTROPHORETIC SEPARATION OF BIOLOGICAL MOLECULES ON MICRO-MACHINED SILICA  
PLATES \ (FINAL REPORT\)

**System Number:**

**Patron Number:**

**Requester:**

**Notes:**

**DSIS Use only:**

**Deliver to:**



# DRES



DEFENCE RESEARCH ESTABLISHMENT SUFFIELD

**CR 97-19**

**UNCLASSIFIED**

## Electrophoretic Separation of Biological Molecules on Micro-machined Silica Plates (Final Report)

BY:

Prof. D. Jed Harrison  
University of Alberta

SUBMITTED TO:  
SCIENTIFIC AUTHORITY

Dr. William Lee  
Defence Research Establishment Suffield  
Box 4000, Medicine Hat, Alberta, T1A 8K6

June 1997

**WARNING**

"The use of this information is permitted subject to recognition of proprietary and patent rights."



CRAD



**Electrophoretic Separation of Biological Molecules on  
Micro-machined Silica Plates**

**Contract No. W7702-4-R444/01-XSG**

**Final Report to DRES**

**DRES SA  
Dr. William Lee  
Chemical Biological Defence Section  
P.O. Box 4000  
Medicine Hat, AB T1A 8K6**

**CONTRACTOR  
Prof. D. Jed Harrison  
University of Alberta  
Department of Chemistry  
Edmonton, AB T6G 2G2**

The principal goals of this project during the funding period were to demonstrate the separation of the products of immunological reactions and of DNA binding assays on a microchip. After achieving this result we were to integrate one of these two classes of reaction onto a chip, along with the separation itself. Electroosmotic flow was to be used to control the fluid flow and pumping within the chip. The choice of which reaction to demonstrate was to be made at the end of the first year, largely based on the success with each type of separation at that time. The report below describes our results.

As a brief summary we were able to demonstrate immunoassay separations of the biological warfare simulant phage virus MS-2, and of small molecule antigens used as drugs, specifically theophylline. Separation of DNA samples obtained from BW simulants, following reaction with a fluorescent probe molecule, was also shown. On-chip reactions and separations were demonstrated for the immunological determination of theophylline.

Our results demonstrate that electrokinetic pumping and control of immuno and DNA assay reagents is possible within a microchip. The quality of results was high, indicating the device could be used in principle for automated BW agent determination.

The data we obtained is presented in three sections below; the first a discussion of immunological separations, the second presenting DNA separations and the third describing immunoreactions and separations integrated on-chip.

## IMMUNOLOGICAL SEPARATIONS

Microfluidic devices etched in glass substrates provide a fluidic network in which chemical reactions, sample injection and separation of reaction products can be achieved. The application of high voltages to conductive fluids within these channels leads to electroosmotic and/or electrophoretic pumping, providing both mass transport and separation of components within the samples. This method pumps fluid at velocities up to 1 cm/s in approximately 20  $\mu\text{m}$  diameter capillaries, while also controlling the direction of fluid flow at capillary intersections, without a need for valves or other moving parts. Electrophoretic effects lead to separation: i.e. the differing mobilities of ions result in different migration rates within an electric field, giving rise to separations.

Integrated devices for chemical separation employed in this study are based on capillary electrophoresis (CE), a method in which high applied voltages can be used to separate the components of a sample with high efficiency. Figure 1 illustrates the layout of the fluid channels in the chip used for these studies. Sample is introduced through a side channel and driven towards sample waste with 500 to 1500 V, creating a 60-100 pL plug of solution at the

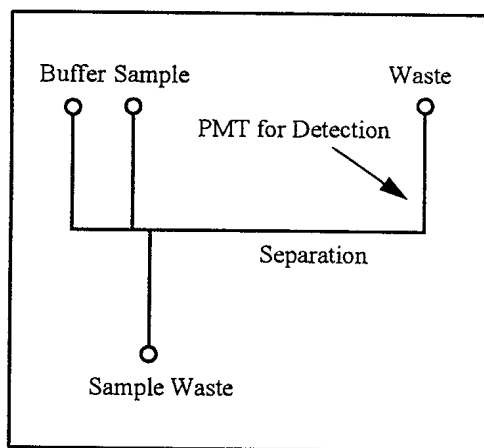


Figure 1. Layout of the flow channels used for immunoassay and DNA chips.

intersection, which can be injected into the separation channel. Fluorescence - detection is used with a 488 nm laser excitation source and a photomultiplier tube for detection of the emission from fluorescently labelled molecules. This detection system is highly selective, as only fluorescent compounds will be observed [1].

Sensitivity is a key issue in immunoassays, as most of the compounds of interest are present at very low concentrations. We improved detection substantially, by optimizing the wafer bonding process to reduce formation of light scattering centers on the surface of the glass devices. Careful alignment of the laser beam to eliminate scatter from the curved walls of the channels was also beneficial. In this way we have

reduced our previous detection limits from about 2 nM down to 30 pM in fluorescein. Detection limits in the pM range are satisfactory for a number of immunoassays.

Solution phase reactions of an antibody (Ab) and its target molecule, the antigen (Ag), are much more rapid than immunosorbent reactions due to the improved mass transfer kinetics of homogeneous reactions. By labelling either the Ag or the Ab with a fluorescent tag, it is possible to determine when a complex between antibody and antigen has been formed, if the products can be separated from the reactants. (We will designate labelled compounds with a \*.) Figure 2 shows an on-chip separation of a labelled antibody (Ab\*) before and after reaction with its antigen. In this case the antigen is the virus MS-2, while the immunoglobulin G (IgG) antibody is fluorescently labelled anti-MS-2. The complexes formed between the two compounds have a different charge to size ratio than either of the free compounds, so they migrate at different rates in the electric field. The unlabelled virus can be determined from the complex it forms with the antibody, while the remaining free antibody is separated from the reacted material.

It is also of great interest to analyze for small molecules by immunoassay methods. A typical example is an analysis for a therapeutic drug for asthma, theophylline (Th). In order to get good separations by CE when using small target molecules, it is necessary to label the analyte molecule instead of the antibody. Labelled Th (Th\*) is thus mixed with a sample containing unlabelled Th, and the two are allowed to compete for a limited amount of antibody to Th, as illustrated in the scheme below.

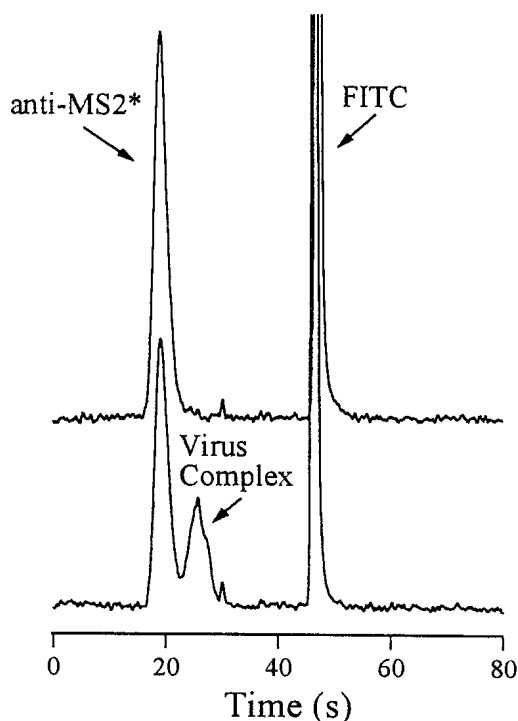
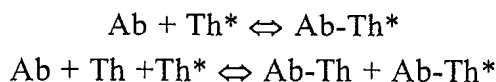


Figure 2. Electropherograms of labeled anti-MS2 IgG alone, and anti-MS2 mixed with the virus.



A competitive assay leads to an increase in signal for the free, labelled  $\text{Th}^*$  as  $\text{Th}$  from a sample increases in concentration. There is a corresponding decrease in signal from the  $\text{Ab-Th}^*$  complex. Figure 3 shows a series of separations performed on-chip in which increasing amounts of  $\text{Th}$  in a sample were added to a fixed amount of  $\text{Th}^*$  and  $\text{Ab}$ . The separation occurs in less than 1 minute and the complex is well resolved from free  $\text{Th}^*$ .

Data like that in Figure 3 provides a calibration curve, such as is shown in Figure 4. Competitive assays of this type are well known to give non-linear calibration curves, but are extensively utilized in clinical diagnostics. To meet therapeutic criteria, serum samples should contain  $\text{Th}$  in the range of 10-20  $\mu\text{g/ml}$ . The lower axis shows the original sample concentrations before dilution, and it is clear that high sensitivity is attained in the therapeutic range. It is common to dilute the serum sample before analysis, and in this study we used a 200-fold dilution factor. The upper axis shows the actual concentration in the measured samples, after dilution.

In the microchip format it is possible to observe both disappearance of the complex and appearance of free  $\text{Th}^*$ . This process leads to greater precision of measurement. Both traces are shown in Figure 4. By measuring both components and recognizing that the total fluorescence signal should remain a constant, it is possible to normalize the signals. This compensates for small variations in the amount of material injected and gives better precision. The y-axis in Figure 4 is thus a plot of peak area for one of the two fluorescent species, ratioed to the total fluorescent signal.

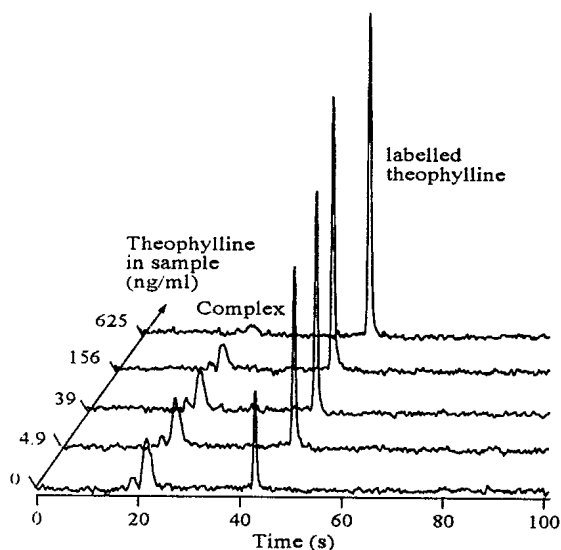


Figure 3. Competitive immunoassay of theophylline performed on-chip. Peaks for the complex and for free  $\text{Th}^*$  are seen. The ratio of peak areas changes as  $\text{Th}$  from a sample is added.

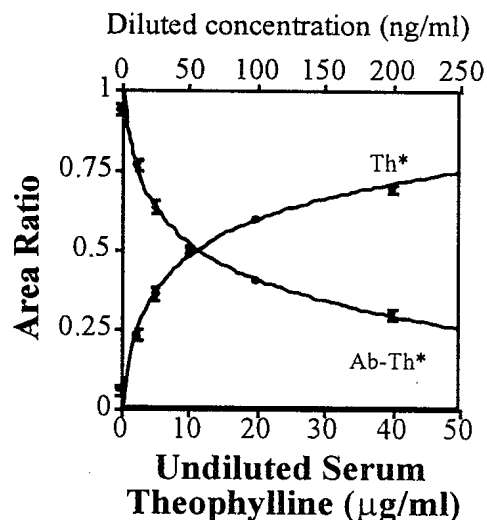


Figure 4. Calibration curve for unlabelled  $\text{Th}$  in a sample. Lower axis shows concentrations before dilution, upper axis shows concentrations after dilution.

The calibration curve illustrates that we are readily able to measure theophylline in the therapeutic range, and that the absolute concentrations measured are in the ng/ml range. The precision of the measurements is within 5%, indicating good analytical performance.

## DNA SEPARATIONS

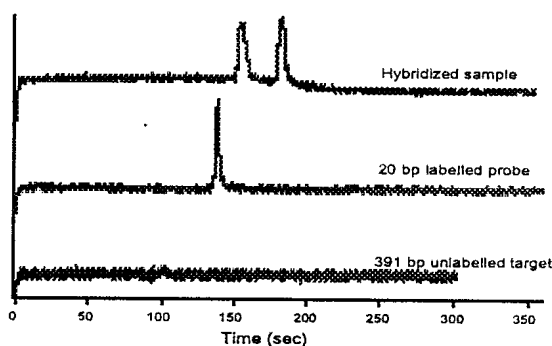
Several groups have already utilized microfabrication to produce DNA analysis systems [2-5]. These systems range from rapid analysis of restriction digests [5] to integration of on-line pre-separation treatments on the chips. On-chip restriction enzyme digest assays [3], hybridization assays [2], and a silicon polymerase chain reaction (PCR) amplification chip coupled with a separation chip [4] have appeared in the literature during the course of this project.

Amplification is a common pre-separation step in DNA analysis. PCR is the most common and a very powerful amplification technique, however there are limitations due to large temperature ranges during cycling, surface chemistry issues, and problems with bubble formation. An alternative method for amplification is Cycling Probe Technology (CPT) [6]. This technique is very amicable to integration with the chips as it involves a single enzyme, gives linear amplification of signal, and is isothermal. Quantitation is easier, no expensive thermocyclers are required, surface chemistry issues are reduced and the signal amplification is very specific. For these reasons DRES selected the CPT assay for our development as an on-chip assay. The first key requirement we needed to demonstrate was that the product separations could be performed on-chip.

## **Experimental**

HPMC, HEC, 1xTBE, urea, fluorescein (Na salt) (Sigma), fluorescein labeled 20 base hybridization probe, and 391 basepair target for Newcastle Disease (Defense Research Establishment Suffield), 12 (5' fluorescein labeled, dA<sub>10</sub>-rA<sub>2</sub>) and 24 base fragments (dA<sub>10</sub>-rA<sub>4</sub>-dA<sub>10</sub>), (ID Biomedical).

The fabrication of the devices in mask glass, power supplies used and optics for detection are described elsewhere. The channels for DNA separation were coated using a slight modification of the Hjerten procedure [8]. The channels were filled with the gel using either vacuum or high pressure.



## **Results and Discussion**

### Hybridization Assays

The chip separation format was evaluated by separation with a model

*Figure 5. Hybridization assay (top) of nonlabeled, PCR amplified, 391 base pair target DNA (bottom) and a fluorescently tagged 20 base probe (middle). 0.4% HPMC gel filled channel, 1xTBE buffer (pH 8.0), 150 V/cm field strength.*



system. A fluorescein tagged probe was conventionally hybridized to a PCR target off-line and the duplex and excess probe separated and detected using the chip. 20 nM of a 20 base probe was mixed with 50 pM of a complimentary, PCR amplified 391 bp sample. The solution was hybridized at 60°C for 10 minutes, loaded onto the chip, injected into the separation channel, and the separation performed. Figure 5 shows the resulting electropherograms of an injection of target DNA only, probe only, and hybridized sample. The target shows no signal increase over background as the target was not fluorescently labeled. The probe trace contains the expected one peak, while the hybridized sample results in an early peak corresponding to excess probe as well as signal from the larger complex or annealed product. Some instability in migration times was observed, as seen in the Figure.

### CPT Separations

The chimeric probes best suited to CPT are relatively short, due to the need to operate at low enough temperatures that the enzyme is not destroyed, while still obtaining good reaction rates. However, separation of short DNA fragments requires careful optimization of experimental parameters. A set of synthetically produced CPT products were used to evaluate separation conditions and to determine the analysis range of the chip compared to conventionally used radioactive detection. Figure 6 shows the separation of a

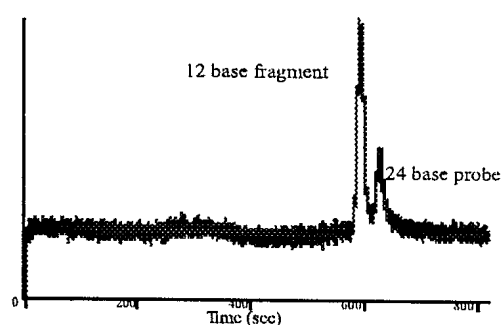


*Figure 6. Separation of synthetic CPT assay products. The original chimeric probe of 14 bases and the 12 base fragments.*

24 base long intact chimeric probe from its 12 base fragment. A gel of 4% HEC in 1xTBE 7M Urea buffer (pH 8.0) was successful, when using 212 V/cm separation field strength.

The determination of target DNA concentration eventually requires a wide dynamic range. Small probe fragment peaks due to low target concentrations may need to be quantified in the presence of a large excess of unreacted probe. On the other hand, high target concentrations drive the reaction to completion, so unreacted probe must be determined with a large excess of fragment present. Figure 7 shows a calibration/dynamic range plot with synthetic mixtures of probe and fragment to determine the dynamic range afforded by the chip separation. The concentration of the 12 base fragment was held constant at 5 nM (and used as an internal standard) while the intact probe concentration was varied. Figure 8 shows the opposite case, the concentration of the 24 base probe was constant (5 nM) while the probe fragment concentration was varied. For this system, the extremes of the dynamic range were limited by the obtainable detection sensitivity as well as the separation resolution.

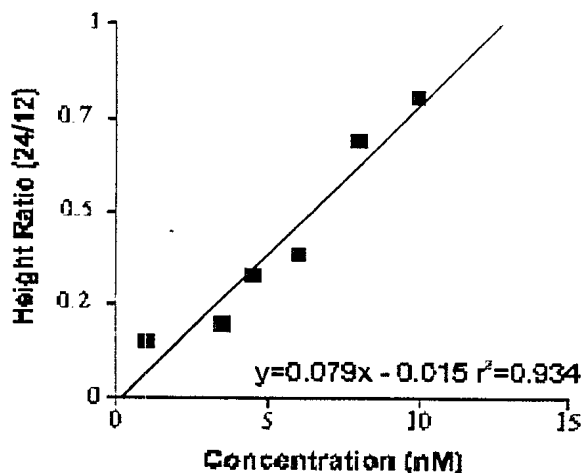


Figure 7. Calibration curve for the separation of synthetic CPT amplification products. Varying concentrations of 24 base probe while the concentration of fragment is constant at 5 nM.

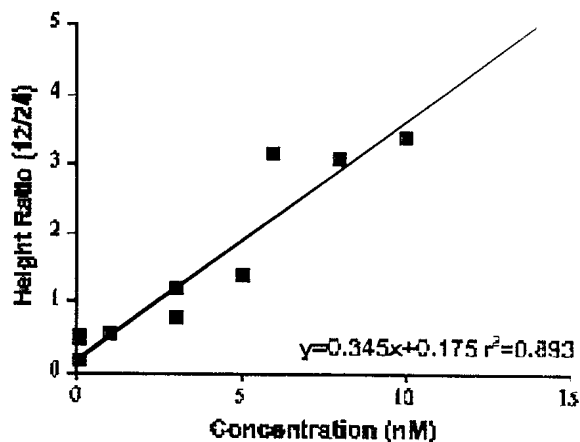


Figure 8. Varying concentration of 12 base fragment probe while the concentration of intact probe is held constant at 5 nM.

## ON-CHIP IMMUNOREACTION AND SEPARATION

In this report we demonstrate that on-chip mixing of diluted serum samples with a labelled tracer compound and a selective antibody can be followed by separation and analysis of the components. This result, shown for the drug theophylline, provides confirmation that the integration of several steps to create a lab-on-a-chip for an immunoassay of complex, real samples is indeed feasible [10-12].

### Experimental

Devices were fabricated in 7.6 x 7.6 cm square Borofloat glass using microlithographic patterning technique and an HF/NO<sub>3</sub> etchant as previously described [8,10,13]. The chip layout is shown in Figure 9. The solution reservoirs are numbered from 1 to 7 for identification.

The "tricine" buffer contained 50 mM tricine adjusted with sodium hydroxide to pH 8.0, 0.01% w/v Tween 20, and 26 mM NaCl [10]. For competitive theophylline assays, serum theophylline (Th) standards from the TDx calibrator kit (0, 2.5, 5.0, 10, 20, 40 µg/ml) were used as received. Samples were made by spiking theophylline into human serum to give solutions 10, 12.5 and 15 µg/ml in theophylline. Standard or sample solutions were then diluted 50x in tricine buffer. Solution T containing the fluorescein labeled theophylline (Th\*) tracer was diluted with the tricine buffer in a 1:1 ratio (V/V). Solution S containing anti-theophylline (Ab) was dialyzed and reconstituted in the tricine buffer as previously described [10], then 2.5 µl of this solution was further diluted with tricine buffer to 40 µl before use.

10 µl of diluted theophylline sample or standard, Tracer Th\*, and anti-theophylline solution were added to reservoirs 5, 6 and 7, respectively as indicated in

Figure 9. Tricine buffer was added to all other reservoirs. Sample reservoirs (5, 6, 7) were connected to ground while sample waste (3) was connected to a negative high voltage (-3 to -6 kV). On-chip mixing of the solution streams and reaction of reagents took place in the mixing coils. The channel segment between junctions J1 and J3 was used to mix the antigens (theophylline and tracer) while the segment between J3 and J4 was used to mix the antigens with the antibody. The mixed solution passed through the double T injector, thereby forming a plug of mixed sample and Ab about 100  $\mu\text{m}$  in length ( $\sim 100$  pL).

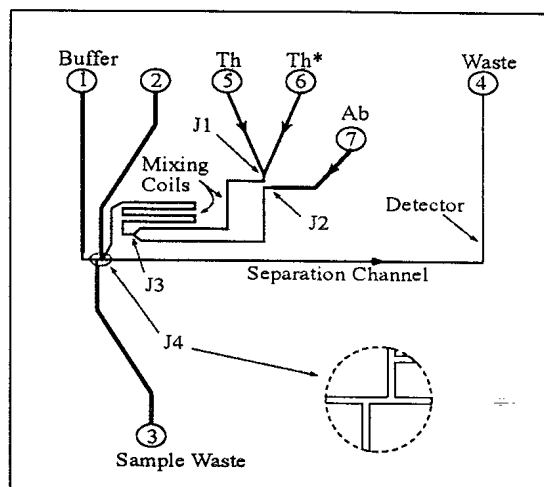


Fig 9. Device layout for competitive immunoassay, showing numbering scheme for solution reservoirs and junctions. Differing line thicknesses indicate relative channel widths. The segment joining J1 to J3 was used for mixing of antibody (Ab) with the antigen and tracer. The double T injector is shown in the inset. The drawing is not exactly to scale.

## Results and Discussion

The mixing manifold illustrated in Figure 9 was designed to premix sample and Th\* tracer in a 1:1 ratio, then mix the resulting solution with Ab, also in a 1:1 ratio. The intention was to apply the same potential to each reservoir and let the geometry of the channels control the mixing ratios.

### Mixing dilution ratio.

The volume flow rate of solution at each of the junction points in the mixing manifolds was designed to be equal, by ensuring equal resistivities and equal cross-sectional areas at each of the mixing junctions [14]. Figure 10 shows electropherograms resulting from on-chip dilution of Th\* at the J3 mixing point. In Figure 10a, reservoirs 5, 6 and 7 all contained the same Th\* solution, while in Figure 10b reservoir 7 contained buffer instead. The latter configuration should give a 50% dilution of the Th\*. In Figure

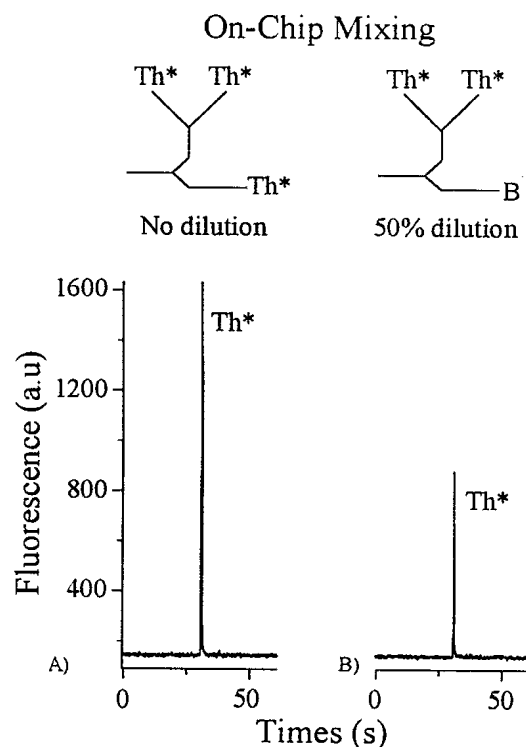


Figure 10. On-chip dilution of tracer Th\* as detailed in the text. A) Th\* was present in reservoirs 5, 6 and 7 and was loaded into the double T injector at -3 kV. B) the Th\* solution in reservoir 7 was replaced with buffer, leading to a 1:1 dilution of the Th\* at the double T injector during loading. For separation and detection, a pH 8.0, tricine buffer was used, with 6 kV between reservoirs 1 and 4.

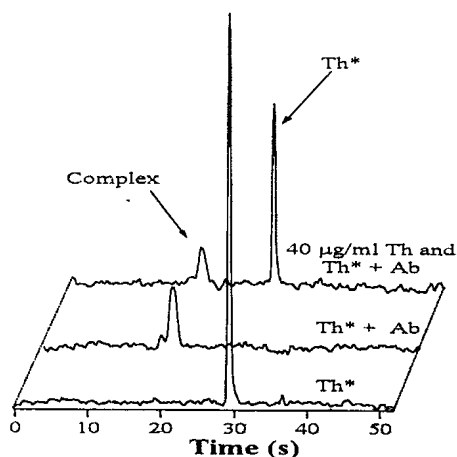


Figure 11. Electropherograms of the competitive theophylline assay with on-chip mixing of reagents. Lower trace with buffer in reservoir 5, Th\* in 6 and buffer in 7; middle trace with buffer in 5, Th\* in 6 and Ab in 7; upper trace with a 40 µg/ml theophylline sample (prior to off-chip 50x dilution) in reservoir 5, Th\* in 6 and Ab in 7. Buffer and separation conditions were the same as for Figure 10.

10a the area under the Th\* peak was  $490 \pm 9$  mV\*s (mean and SD for 4 replicates (n)), while in Figure 10b dilution resulted in an area of  $236 \pm 4$  (n = 7). This corresponds to a Th\*:buffer ratio of  $48.2 \pm 1.2$  %. Mixing both on- and off-chip was also compared. The ratio of the dilution achieved on-chip to that off-chip was  $103 \pm 7$  %. In this study we used a simplified potential delivery system, with a single fixed voltage applied to each of the delivery reservoirs, but greater control of mixing is clearly possible if the potentials on each of those reservoirs is varied [14]. Consequently, slight differences in mixing ratio between design and result can be readily compensated.

### Immunoreactions On-Chip

Figure 11 shows electropherograms obtained for on-chip competitive immunoassays of serum theophylline. Mixing was performed at -6 kV under continuous flow conditions to give about 32 s reaction times, followed by separation at -6 kV. For the lower trace, Th\* alone was injected to give a single fluorescence peak at about 30 s. The central electropherogram was obtained following on-chip mixing of a diluted blank theophylline (0 µg/ml) serum sample in reservoir 5 with tracer Th\* from 6, then with anti-theophylline from 7. The Th\* was completely bound to anti-theophylline to form complexes, which were detected as a new pair of partially resolved peaks at about 18 s. Competitive assays were achieved by replacing the blank sample in reservoir 5 with diluted serum theophylline solution. The separation was completed in less than 1 minute, the bound Th\*-antibody complexes were well resolved from the free Th\* and the peak areas were easily quantitated.

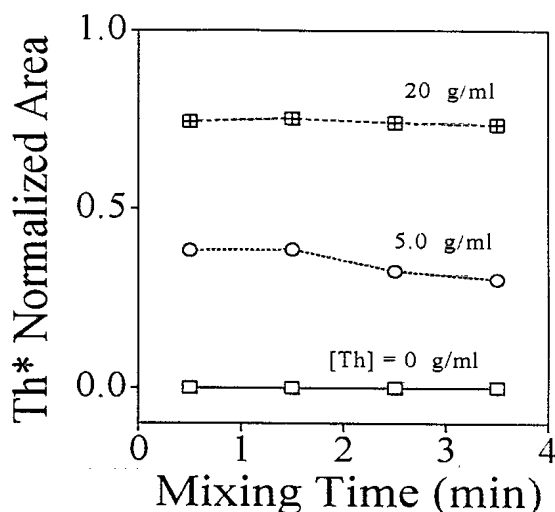


Figure 12. Stop-flow study of the effect of mixing time on the amount of free, unreacted Th\* in the presence of Ab and the indicated amounts of unlabelled Th (concentrations reported as the value prior to 50x dilution off-chip). The mixed Ab, Th\* and Th solutions were allowed to sit in the channel segment between J3 and J4 for varying periods. The shortest mixing time corresponds to the minimum possible residence time, given the velocity of flow with -6 kV applied to the sample waste reservoir.

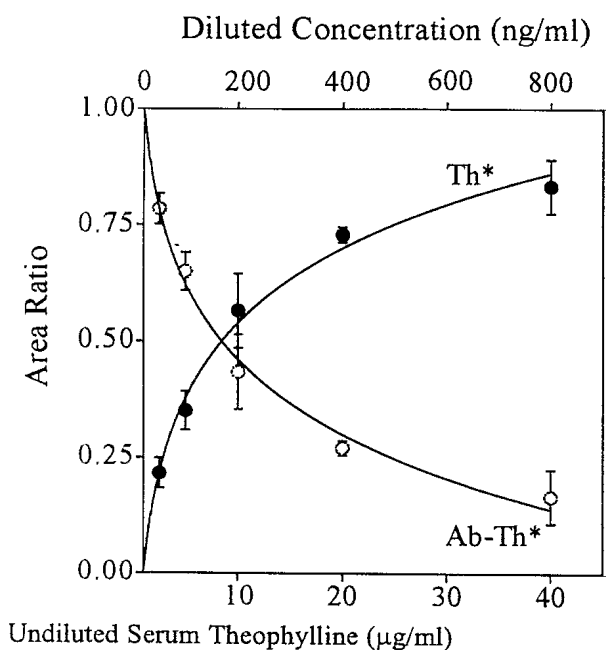


Figure 13. Calibration curve of normalized peak area for (●) free Th\* and (○) Ab-Th\* complex vs. concentration of Th in 50x diluted serum standards (upper axis). Lower axis shows Th concentrations as they were in serum standards before 50x dilution off-chip. Buffer and separation conditions were the same as for Figure 10. Each point is the mean of 4 replicates. Error bars show the standard deviations where they were larger than the data points. Solid lines are fits to a log function; see text.

#### Competitive Theophylline Assays On-Chip

Figure 13 shows a calibration curve obtained from a series of separations, in which varying concentrations of diluted serum theophylline standards were mixed on-chip with Tracer Th\* and anti-theophylline solutions. The chip was operated in stop-flow mode, allowing reaction times of 32, 90, 150, and 210 s. A plot of normalized peak area for Th\* (averaged over all reaction times) versus log[theophylline] was linear (slope =  $0.54 \pm 0.03$ , intercept =  $0.003 \pm 0.04$ ), and allowed calculation of the solid line shown in Figure 13. The lower axis of Figure 13 shows the original concentrations of Th in the serum standards, while the upper axis shows the concentrations of the standards at the stage they were added to reservoir 5. The calibration curve covers the important clinical range of 10-20 µg/ml for serum samples. It is similar to those obtained with on-chip analysis of off-chip mixed samples or with the FPIA method.

The recovery of theophylline from spiked human serum samples run over a two day period. Human serum samples with theophylline at 10, 12.5, and 15 µg/ml were found to have  $9.4 \pm 1.0$ ,  $12.9 \pm 1.8$  and  $17 \pm 2$  µg/ml, respectively, (mean and SD over 4 replicate injections) when the peak areas from the four different reaction times were averaged. The precision of the recovery results obtained with on-chip mixing is poorer than those we obtained with off-chip mixing. This discrepancy appears to arise from averaging data obtained at several different reaction times. When samples and standards

It is possible to increase reaction times by using the chip as a stop-flow mixer, allowing incubation in the mixing coil while there is no flow in the mixer. The volume ratio of the second mixer to that of the injector port (51 vs 0.15 nL) means there will be enough reacted sample available. Figure 12 shows the effect of cumulative mixing time on the distribution between free and bound Th\* in a series of competitive assays with serum theophylline standards at 21° C. Remaining unreacted Th\*, normalized to the total fluorescent Th\* is plotted as a function of total mixing time. The competitive immunoreaction was nearly complete in the first 30 s of continuous flow mixing. A slight continued decrease in free Th\* with increased mixing time at low Th concentration suggests that the reaction continues at a slow rate for an extended period, consistent with the known chemistry of this system [15].

for calibration curves were analyzed at any one of the fixed mixing times, the precision of the recovery improved to, for example,  $16.0 \pm 1.2 \mu\text{g/ml}$  for a  $15 \mu\text{g/ml}$  sample. This improvement leads to a precision for on-chip mixing which is similar to that which we obtained with off-chip mixing [10]. Careful control of the mixing time in both standards and sample testing is required to achieve this, but is not overly difficult given the computer control used to run the chips.

The absolute detection limit (DL) for a solution within the chip's separation channel was determined to be  $1.1 \text{ ng/ml}$ . This is consistent with the value of  $1.25 \text{ ng/ml}$  we obtained for off-chip mixing with separation on-chip. Since the present chip performs a 4-fold dilution, the minimum concentration that can be placed in sample reservoir 5 is  $4.3 \text{ ng/ml}$ . Given the 50x dilution step performed before the samples and standards are introduced to the chip, the on-chip reaction and separation system provides a DL of  $0.22 \mu\text{g/ml}$  for undiluted serum. This value is similar to the  $0.4 \mu\text{g/ml}$  reported for theophylline assay by FPIA [16], serving to illustrate that detection limits are not sacrificed by performing the on-chip immunoassay.

## Conclusions

The research project has met the stated goals of the original contract. Detection limits of small fluorescent molecules were reduced by about 1000-fold during these studies, to a range of 10-100 pM. The detection limits measured for the drug theophylline, as determined by on-chip immunoassay were a few nM, or ng/ml, somewhat better than the limits obtained with conventional methods. These results indicate the detection limits were controlled by the equilibrium binding constant of the immunoassay, rather than by the performance of the chip or the detector. The demonstrated ability to perform sample and reagent mixing on-chip in a controlled fashion, followed by on-chip separation of the reactants, is a strong indicator that the lab on a chip concept is viable for biochemical assays. Since this system is readily automated, the results establish it is a potential candidate for an operator independent detection system in the field, or at the least for operation by staff with minimal training needs. The absolute detection limits are in a very acceptable range, although the detection limits of the immunoassay method might need to be improved. Increased immunoassay sensitivity will depend on the development of antibodies with high affinities, which is certainly feasible. The MS-2 virus assay is of direct relevance to the testing of simulants, as is the DNA assay for the PCR product obtained from Newcastle disease virus. These studies demonstrate the chip can be used with simulant agents as well as with therapeutic drugs, and further that DNA separations of simulant agent DNA assays are possible on-chip. Consequently, the applicability of the microchip concept to simulant analyses is supported by our study.

At present our results must be regarded as highly promising, with the caveat that they represent laboratory based studies. The next stage of development must involve extending the on-chip reactions demonstrated with theophylline to simulants, both in the immuno- and DNA-probe reactions manifolds. Subsequent tests with samples obtained

from field releases of simulants, and later field trials represent the next important steps in establishing and evaluating this promising technology.

## References

1. Albin, M.; Weinberger, R.; Sapp, E.; Moring, S. *Anal. Chem.* **1991**, *63*, 417.
2. Burns, M.A.; Mastrangelo, C.H.; Sammarco, T.S.; Man, F.P.; Webster, J.R.; Johnson, B.N.; Foerster, B.; Jones, D.; Fields, Y.; Kaiser, A.R.; Burke, D.T. *Proc. Nat. Acad. Sci. U.S.A.* **1996**, *93*, (11), 5556-5561.
3. Jacobson, S.C.; Ramsey, J.M. *Anal. Chem.* **1996**, *68* (5), 720-723.
4. Woolley, A.T.; Hadley, D.; Landre, P.; Demello, A.J.; Mathies, R.A.; Northrup, M.A. *Anal. Chem.* **1996**, *68* (23), 4081-4086.
5. Woolley, A.T.; Mathies, R.A. *Proc. Nat. Acad. Sci. USA.* **1994**, *91*, 11348-11352.
6. Duck, P.; Alvarado-Urbina, G.; Burdick, B.; Collier, B. *BioTechniques* **1990**, *9* (2), 142-148.
7. Liang, Z.; Chiem, N.; Ocvirk, G.; Tang, T.; Fluri, K.; Harrison, D.J. *Anal. Chem.* **1996**, *68*, 1040-1046.
8. Fan, Z.H.; Harrison, D.J. *Anal. Chem.* **1994**, *66*, 177-184.
9. Barberi, R.; Bonvent, J.J.; Bartolino, R.; Roeraade, J.; Bapelli, L.; Righetti, P.G. *J. Chromatogr. B.* **1996**, *683* (1), 3-13.
10. Chiem, N.; Harrison, D.J. *Anal. Chem.* **1997**, *69*, 373-378.
11. Koutny, L.B.; Schmaizing, D.; Taylor, T.A.; Fuchs, M. *Anal. Chem.* **1996**, *68*, 18-22.
12. Dirks, J.L.; *AACN Clin. Issues.* **1996**, *7*, 249-259.
13. Fluri, K.; Fitzpatrick, G.; Chiem, N.; Harrison, D.J. *Anal. Chem.* **1996**, *68*, 4285-4290.
14. Seiler, K.; Fan, Z.H.; Fluri, K.; Harrison, D.J. *Anal. Chem.* **1994**, *66*, 3485-3491.
15. Jolley, M.E.; Stroupe, S.D.; Schwenzler, K.S.; Wang, C.J.; Lu-Steffes, M.; Hill, H.D.; Popelka, S.R.; Holen, J.T.; Kelso, D.M. *Clin. Chem.* **1981**, *27*, 1575-1579.
16. Loomis, K.F.; Frye, R.M. *Am. J. Clin. Pathol.* **1983**, *80*, 686-691.

UNCLASSIFIED

~~#506396~~  
506936

UNCLASSIFIED